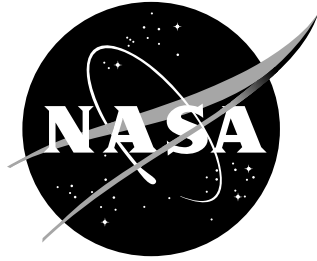


NASA/TM-2002-211676
ARL-TR-2728



Accelerated Near-Threshold Fatigue Crack Growth Behavior of an Aluminum Powder Metallurgy Alloy

Robert S. Piascik
NASA Langley Research Center, Hampton, Virginia

John A. Newman
U.S. Army Research Laboratory
Vehicle Technology Directorate
Langley Research Center, Hampton, Virginia

May 2002

The NASA STI Program Office ... in Profile

Since its founding, NASA has been dedicated to the advancement of aeronautics and space science. The NASA Scientific and Technical Information (STI) Program Office plays a key part in helping NASA maintain this important role.

The NASA STI Program Office is operated by Langley Research Center, the lead center for NASA's scientific and technical information. The NASA STI Program Office provides access to the NASA STI Database, the largest collection of aeronautical and space science STI in the world. The Program Office is also NASA's institutional mechanism for disseminating the results of its research and development activities. These results are published by NASA in the NASA STI Report Series, which includes the following report types:

- **TECHNICAL PUBLICATION.** Reports of completed research or a major significant phase of research that present the results of NASA programs and include extensive data or theoretical analysis. Includes compilations of significant scientific and technical data and information deemed to be of continuing reference value. NASA counterpart of peer-reviewed formal professional papers, but having less stringent limitations on manuscript length and extent of graphic presentations.
- **TECHNICAL MEMORANDUM.** Scientific and technical findings that are preliminary or of specialized interest, e.g., quick release reports, working papers, and bibliographies that contain minimal annotation. Does not contain extensive analysis.
- **CONTRACTOR REPORT.** Scientific and technical findings by NASA-sponsored contractors and grantees.

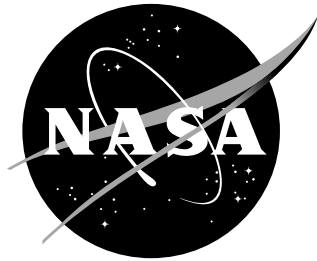
- **CONFERENCE PUBLICATION.** Collected papers from scientific and technical conferences, symposia, seminars, or other meetings sponsored or co-sponsored by NASA.
- **SPECIAL PUBLICATION.** Scientific, technical, or historical information from NASA programs, projects, and missions, often concerned with subjects having substantial public interest.
- **TECHNICAL TRANSLATION.** English-language translations of foreign scientific and technical material pertinent to NASA's mission.

Specialized services that complement the STI Program Office's diverse offerings include creating custom thesauri, building customized databases, organizing and publishing research results ... even providing videos.

For more information about the NASA STI Program Office, see the following:

- Access the NASA STI Program Home Page at <http://www.sti.nasa.gov>
- E-mail your question via the Internet to help@sti.nasa.gov
- Fax your question to the NASA STI Help Desk at (301) 621-0134
- Phone the NASA STI Help Desk at (301) 621-0390
- Write to:
NASA STI Help Desk
NASA Center for AeroSpace Information
7121 Standard Drive
Hanover, MD 21076-1320

NASA/TM-2002-211676
ARL-TR-2728



Accelerated Near-Threshold Fatigue Crack Growth Behavior of an Aluminum Powder Metallurgy Alloy

Robert S. Piascik
NASA Langley Research Center, Hampton, Virginia

John A. Newman
U.S. Army Research Laboratory
Vehicle Technology Directorate
Langley Research Center, Hampton, Virginia

National Aeronautics and
Space Administration

Langley Research Center
Hampton, Virginia 23681-2199

May 2002

Available from:

NASA Center for AeroSpace Information (CASI)
7121 Standard Drive
Hanover, MD 21076-1320
(301) 621-0390

National Technical Information Service (NTIS)
5285 Port Royal Road
Springfield, VA 22161-2171
(703) 605-6000

Abstract

Fatigue crack growth (FCG) research conducted in the near threshold regime has identified a room temperature creep crack growth damage mechanism for a fine grain powder metallurgy (PM) aluminum alloy (8009). At very low ΔK , an abrupt acceleration in room temperature FCG rate occurs at high stress ratio ($R = K_{min}/K_{max}$). The near threshold accelerated FCG rates are exacerbated by increased levels of K_{max} ($K_{max} \geq 0.4 K_{IC}$). Detailed fractographic analysis correlates accelerated FCG with the formation of crack-tip process zone micro-void damage. Experimental results show that the K_{max} influenced accelerated crack growth in the near-threshold regime is time and temperature dependent.

Introduction

In cases where fatigue lives primarily depend on the early stages of crack growth, it is critical to understand the FCG characteristics in the near threshold regime, defined schematically in Figure 1. Considerable research has shown that an acceleration in near threshold FCG rates (da/dN) occurs with increasing stress ratio due to a reduction in crack closure (ref. 1). However, research has suggested that crack closure does not account for all stress ratio effects when R ranges from 0.5 to 0.95, and for K_{max} greater than $0.4 K_{IC}$ (refs. 2 and 3). This work suggests that near threshold FCG can be influenced by other crack-tip damage mechanisms (K_{max} effects) that are not related to crack closure. For ingot metallurgy aluminum and titanium alloys, relatively small near threshold K_{max} effects have been observed during closure free FCG (ref. 3). Others have concluded that highly accelerated near threshold FCG rates during constant- K_{max} testing of low toughness titanium and nickel-based alloys are due to hydrogen assisted cracking (refs. 4-6).

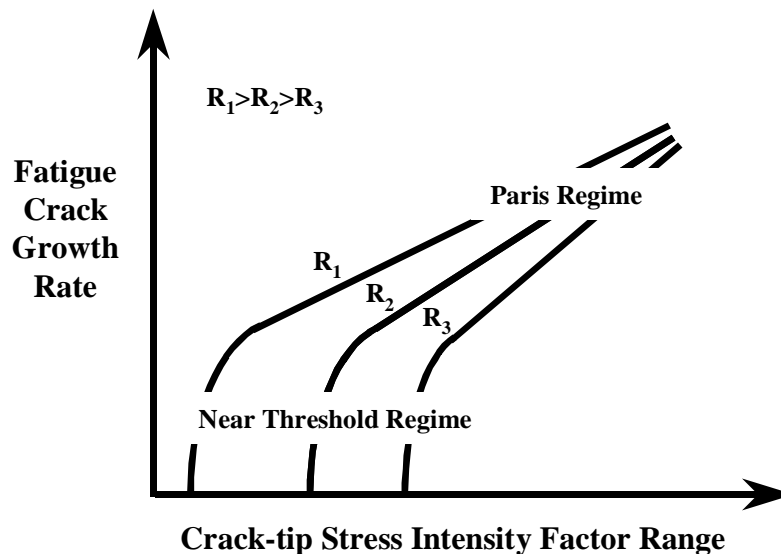


Figure 1. A schematic is shown of the fatigue crack growth rate behavior in the near-threshold and Paris regimes. As the stress ratio (R) is increased, a pronounced increase in fatigue crack growth rate is typically observed in the near threshold regime.

The unusual room temperature near-threshold FCG behavior observed during constant- K_{\max} testing (5.5 and 11 MPa $\sqrt{\text{m}}$) of a powder metallurgy (PM) aluminum alloy (8009) is plotted in Figure 2a (ref. 7). Transitions to accelerated FCG rates (dramatic slope changes in the da/dN versus ΔK data identified with arrows) were correlated with changes in crack surface morphology. For both levels of K_{\max} , a flat fatigue crack surface morphology (micrographs shown in Figures 2c and 2e) was observed at higher levels of ΔK . As ΔK was reduced and accelerated da/dN behavior was observed, the fatigue crack surface abruptly changed to a micro-void morphology (shown in Figures 2b and 2d) similar to that observed during elevated temperature creep crack growth (refs. 8 and 9). The aim of this research is to identify the crack-tip mechanisms that result in accelerated fatigue crack growth in the near-threshold regime.

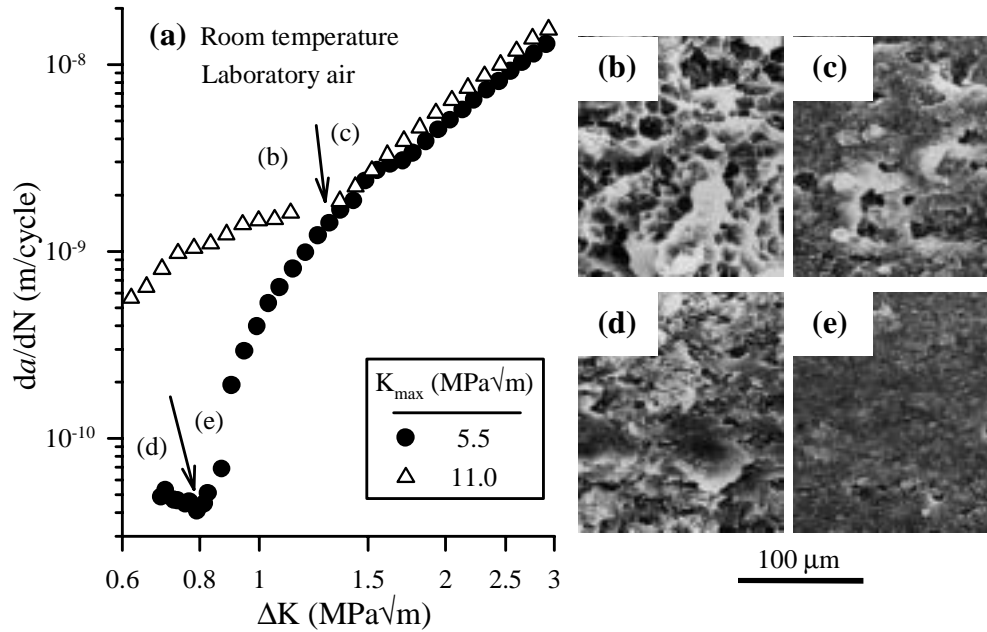


Figure 2. (a) Constant- K_{\max} FCG data for K_{\max} of 5.5 and 11.0 MPa $\sqrt{\text{m}}$ ($f = 11$ Hz). FCG transitions (arrows) mark with changes in crack surface morphology. (b and c) Micro-void crack surface produced at $K_{\max} = 11.0$ MPa $\sqrt{\text{m}}$ and $\Delta K < 1.3$ MPa $\sqrt{\text{m}}$ and a flat surface produced at $\Delta K > 1.3$ MPa $\sqrt{\text{m}}$, respectively. (d and e) Micro-void crack surface produced at $K_{\max} = 5.5$ MPa $\sqrt{\text{m}}$ and $\Delta K < 0.8$ MPa $\sqrt{\text{m}}$ and a flat surface produced at $\Delta K > 0.8$ MPa $\sqrt{\text{m}}$, respectively.

Experimental Procedure

Fatigue crack growth testing was conducted using aluminum alloy 8009; a powder-metallurgy (PM) dispersion-strengthened alloy that was developed to retain high strength at elevated temperatures. The nominal composition of alloy 8009 (in percent by weight is 8.5%-Fe, 1.3%-V, and 1.7%-Si (refs. 8 and 9). This alloy has an extremely fine microstructure with an average grain size for the matrix of approximately 500 nm. $\text{Al}_{12}(\text{Fe}, \text{V})_3\text{Si}$ dispersoids comprise 25 volume percent of the alloy and range in size from 40nm to 80 nm.

Constant- K_{\max} fatigue crack growth tests were conducted in laboratory air, and ΔK was reduced at a K -gradient of $C = -787 \text{ m}^{-1}$ (ref. 10). All tests were conducted using a computer-controlled servo-hydraulic test machine and the K -controlled tests were performed using the ASTM eccentrically-loaded-single-edge-notch tension ESE(T) specimen. Specimens having a width and thickness of 38.1 mm and 2.3 mm, respectively, were fabricated from 8009 aluminum sheet (ref. 11). The back-face strain compliance

method was used to continuously monitor crack length. During the constant- K_{\max} tests, K_{\max} was held constant and increasing K_{\min} and R was used to reduce ΔK . This test procedure results in high values of R in the near-threshold regime, thus eliminating the affects of crack closure (ref. 12). Constant ΔK tests were conducted to determine the affect of loading frequency on FCG. Under constant ΔK conditions, the plot of crack length versus load cycles was used to accurately determine the influence of frequency on da/dN . FCG testing in ultrahigh vacuum (UHV) was conducted in a stainless steel chamber capable of a 1.3×10^{-7} Pa vacuum environment.

Experimental Results and Discussion

Figure 3a shows the near threshold FCG characteristics in UHV at a constant $K_{\max} = 7.7 \text{ MPa}\sqrt{\text{m}}$. The room temperature (297 K) results confirm that the near threshold flat crack to micro-void transition previously observed in room temperature laboratory air (Figure 2) is also observed in inert vacuum environment. Additional vacuum FCG tests were performed under identical fatigue loading ($K_{\max} = 7.7 \text{ MPa}\sqrt{\text{m}}$) and at elevated temperature (339 K and 366 K). The elevated temperature test results and fractographic observations revealed a similar near threshold FCG transition behavior (da/dN_{trans}). The results in Figure 3a show that the FCG transitions occur at higher da/dN with elevated temperature and crack surface observations indicate that the near threshold micro-void cracking was exacerbated by temperature. Similar to the laboratory air results shown in Figure 2a, all vacuum FCG rate data nearly collapse to a single temperature-independent curve ($da/dN|_{297 \text{ K}} = da/dN|_{339 \text{ K}} = da/dN|_{366 \text{ K}}$) where flat crack morphology is observed for $da/dN > (da/dN_{\text{trans}})$. The time-based transition crack growth rate, $\log(da/dt_{\text{trans}})$, is plotted versus the reciprocal of test temperature ($1/T$) in Figure 3b. The linear Arrhenius behavior shown in Figure 3b suggests that a single time and temperature dependent mechanism is responsible for the near threshold micro-void crack growth behavior.

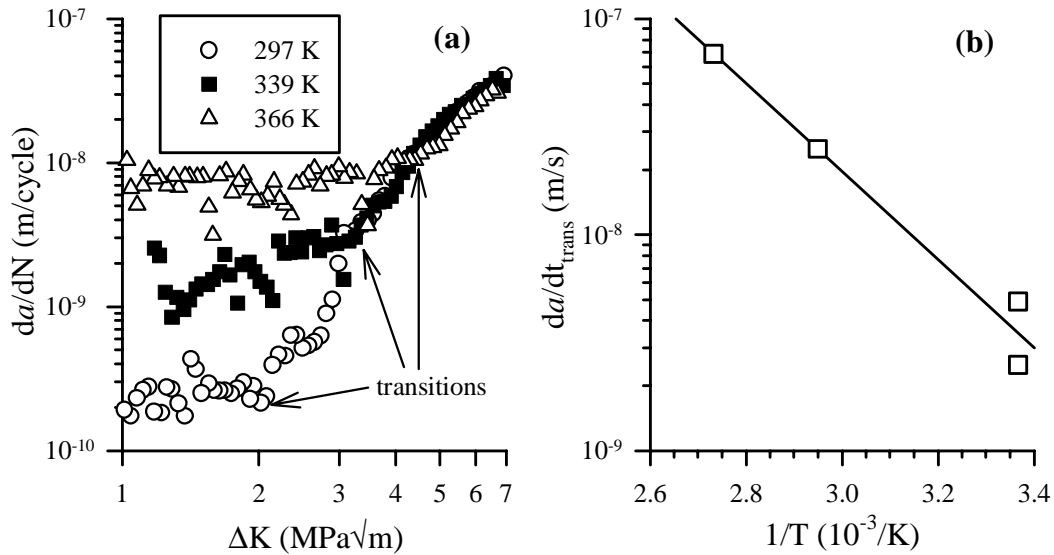


Figure 3. (a) Ultra high vacuum constant- $K_{\max} = 7.7 \text{ MPa}\sqrt{\text{m}}$ FCG data ($f = 10 \text{ Hz}$) are shown for three temperatures (297 K, 339 K, and 366 K). (b) Shown is an Arrhenius plot of transition (time dependent) crack growth (da/dt) versus temperature ($1/T$).

Constant ΔK FCG testing was conducted to show that the near threshold micro-void crack growth described in Figure 3 is related to a time dependent damage mechanism. Figure 4 shows the results of laboratory air FCG experiments conducted at a constant $\Delta K = 0.77 \text{ MPa}\sqrt{\text{m}}$ and three different loading

frequencies (11 Hz, 5 Hz, and 1 Hz). Testing was performed at a $K_{\max} = 5.5 \text{ MPa}\sqrt{\text{m}}$ to ensure that crack growth was conducted within the accelerated FCG regime identified in “region-d” of Figure 2a. The plot of crack length versus load cycle (N) in Figure 4a reveals an increase in micro-void FCG rate with decreased loading frequency; here, the constant FCG rate, linear slope ($\Delta a/\Delta N$), was calculated for each loading frequency (f). Room temperature FCG rates for ΔK levels greater than the da/dN transition (flat crack morphology) shown in Figures 2 and 3 are independent of frequency (ref. 7). Figure 4b shows the constant ΔK data plotted as crack length versus time (t), where $t = (N)(f)$. The near linear slope shown in Figure 4b shows that the near threshold phenomenon is the result of a time dependent crack growth mechanism. Identical constant ΔK tests, not reported here, were also conducted in inert vacuum; similar time dependent crack growth behavior was observed in the UHV environment. The UHV results show that the laboratory air frequency effect was not the result of crack-tip environment interactions.

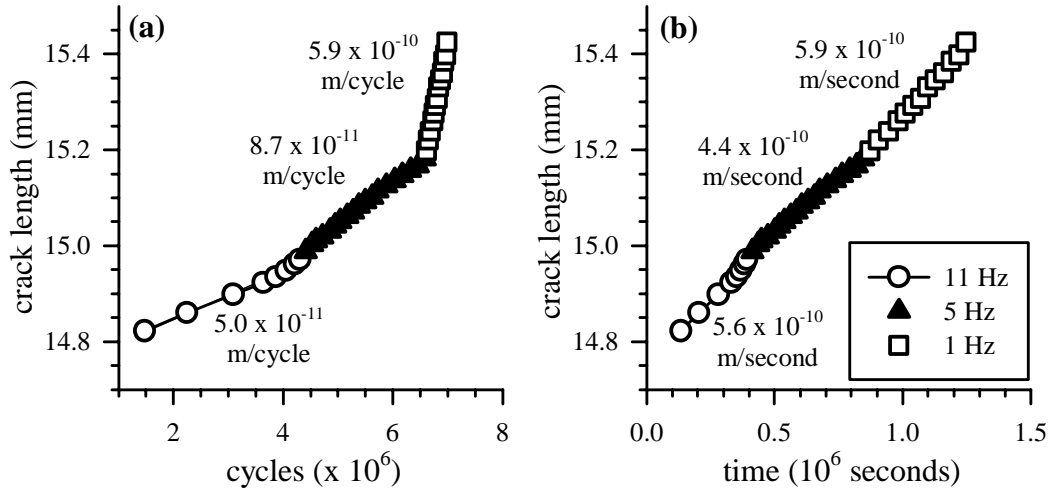


Figure 4. (a) Laboratory-air, room-temperature constant $\Delta K = 0.77 \text{ MPa}\sqrt{\text{m}}$ FCG test results ($K_{\max} = 5.5 \text{ MPa}\sqrt{\text{m}}$) conducted at 11 Hz, 5 Hz, and 1 Hz. The change in slope shows a distinct increase in FCG rate (da/dN) with decreased load frequency. The same data are plotted in (b) as crack length versus time; a constant crack growth rate (per unit time), da/dt is observed.

A series of static load tests were conducted to show that the near threshold micro-void crack growth phenomenon is the result of room temperature creep. Here, the test load was selected to create an initial crack-tip stress intensity factor ($K = 5.5 \text{ MPa}\sqrt{\text{m}}$) that was identical to the value of K_{\max} that produced micro-void crack growth during near threshold FCG testing (refer to Figure 2). No visible crack growth was observed on the specimen surface during these constant load tests. However, because micro-void crack growth was limited to the specimen interior (crack tunneling) during constant- K_{\max} fatigue testing (ref. 7), it was suspected that constant-load crack growth might also be limited to the specimen interior. To investigate the tunneled crack growth behavior, a series of tests were conducted under static load conditions with intermittent fatigue; here, intermittent fatigue loading was used to produce a characteristic fatigue crack surface that marked the regions of constant load cracking. The micrographs in Figure 5a and 5b show the fracture surface of specimen that was pre-cracked by fatigue loading at a constant $\Delta K = 5.5 \text{ MPa}\sqrt{\text{m}}$ ($K_{\max} = 11.0 \text{ MPa}\sqrt{\text{m}}$, $R = 0.5$ and $f = 10 \text{ Hz}$); these test parameters resulted a relatively straight crack front (dashed line). Fatigue pre-cracking was stopped after a steady-state FCG rate was established. Following the pre-crack, a static load corresponding to the maximum fatigue load ($K = 11.0 \text{ MPa}\sqrt{\text{m}}$) was maintained for a specified time. After each static load test, fatigue loading (pre-crack parameters) was resumed until steady-state FCG rate conditions were reached to (1) mark the final static load crack front (solid line in Figures 5a and 5b) and (2) reestablish a straight fatigue crack front for the next static load test. A total of eight static load tests were performed maintaining the prescribed load for

different time intervals ranging from 1 hour to 120 hours. Examination of the resulting crack surface revealed a change in crack surface morphology during the static load tests. Figures 5a and 5b are micrographs that show the crack surface produced during static loading for 43 hours and 10 hours, respectively. The light colored regions bounded by the dashed line (fatigue pre-crack front) and the solid line (tunneled static load crack front) is the region of constant load cracking. Detailed SEM examinations revealed that all eight static load crack surfaces exhibited the same micro-void morphology and crack-tunneling configuration observed during near threshold FCG testing (Figure 2b). The tunneled crack configuration required for micro-void crack growth indicates that the time and temperature dependent damage mechanism is a plane-strain (triaxial state of stress) induced damage mode that is characteristic of creep crack growth. The plot of tunneled (centerline) crack length (Δa) versus test time (t) for the eight static load tests (Figure 5c) shows that room temperature creep crack growth rates are similar to the growth rate of near threshold micro-void cracking. The dashed line in Figure 5c represents the micro-void crack growth rate ($da/dt = 2.05 \times 10^{-8}$ m/s) that corresponds to the “b/c - FCG transition” in Figure 2a where early stages of micro-void (tunneled) crack growth are likely. The similar slope of the dashed line and the average creep crack growth rate during the early stages of tunneled crack growth (linear regression for $\Delta a < 1$ mm, solid line) indicate that the accelerated near threshold fatigue crack growth rates shown in Figures 2 and 3 are the result of a creep dominated crack growth mechanism.

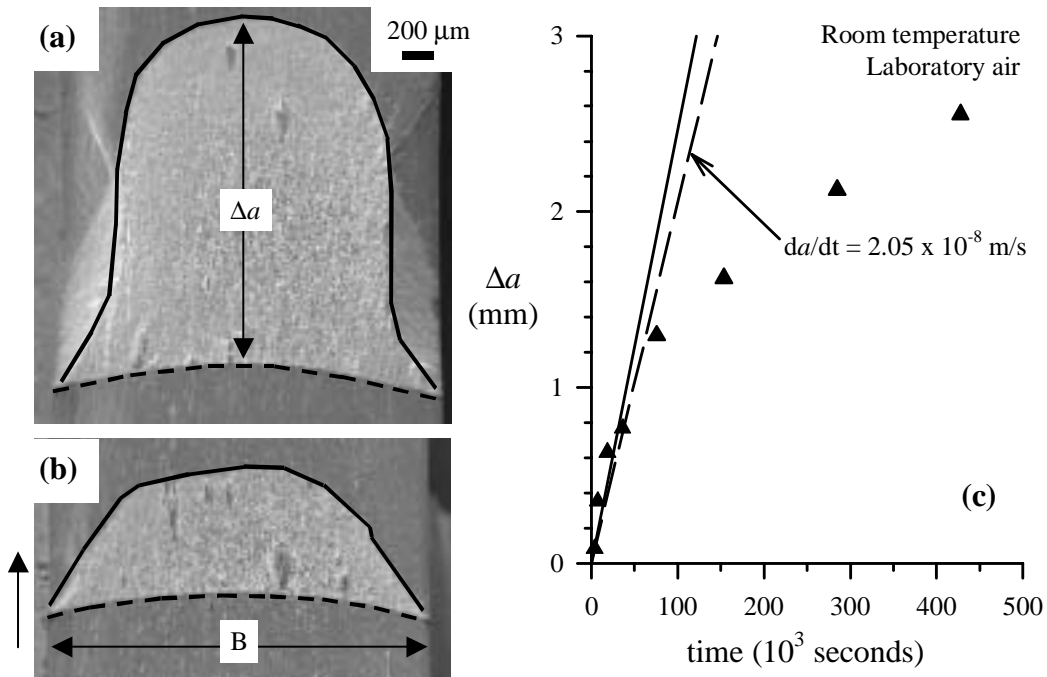


Figure 5. (a and b) Shown are tunneled crack surface produced by constant load time dependent crack growth during a 43-hour test and 10-hour test, respectively. The specimen thickness is “B” and direction of crack growth (arrow, \uparrow) is noted. (c) The plot shows crack growth at the specimen centerline, Δa , versus time for eight experiments performed at times ranging from 1 hour to 120 hours

Conclusions

Results show that the near threshold accelerated fatigue crack growth observed in aluminum alloy 8009 is the result of a room-temperature creep dominated damage mechanism. The micro-void crack growth mechanism requires a high local triaxial state of stress (plane-strain specimen interior) and elevated K_{\max} levels ($K_{\max} > 0.4 K_{IC}$) during fatigue loading.

The room temperature creep mechanism was only observed in the near threshold regime at elevated levels of mean stress. Consequently, the constant K_{\max} test procedure was critical in identifying and characterizing the near threshold phenomenon.

References

- [1] J. C. Newman, Jr. and W. Elber (editors), *Mechanics of Fatigue Crack Closure*, ASTM STP 982, American Society for Testing and Materials, Philadelphia, PA, 1988.
- [2] D. Gan and J. Weertman, "Crack Closure and Crack Propagation Rates in 7050 Aluminum," *Engineering Fracture Mechanics*, Vol. 15, 1981, pp. 87-106.
- [3] C. Beevers, "Fatigue Crack Growth Characteristics at Low Stress Intensities of Metals and Alloys," *Metals Science*, August/September 1977, pp. 362-367.
- [4] G. Marci, "Failure Mode Below 390K with IMI 834," *Proceedings of the 6th International Fatigue Conference*, Berlin, Germany, Vol. 1, 1996, pp. 493-498.
- [5] M. Lang, G. Hartman, and J. Larsen, "Investigation of an Abnormality in Fatigue Crack Growth Curves-The Marci Effect," *Scripta Materialia* Vol. 38, 1998, pp. 1803-1810.
- [6] M. Lang, "Explanation of an Apparent Abnormality in Fatigue Crack Growth Rate Curves in Titanium Alloys," *Acta Materialia*, Vol. 47, 1999, pp. 3247-3261.
- [7] J. A. Newman, W. T. Riddell, and R. S. Piascik, "Effects of K_{\max} on Fatigue Crack Growth Threshold in Aluminum Alloys," *ASTM STP 1372*, American Society for Testing and Materials, West Conshohocken, PA, 2000, pp. 63-77.
- [8] K. Jata, D. Maxwell, and T. Nicholas, "Influence of Environment and Creep on Fatigue Crack Growth in a High Temperature Aluminum Alloy 8009," *Journal of Engineering Materials and Technology*, Vol. 116, 1994, pp. 45-53.
- [9] S. Claeys, J. Jones, and J. Allison, "A Fractographic Study of Creep Crack Growth in Rapidly Solidified Al-Fe-X Alloys," *Dispersion Strengthened Aluminum Alloys*, Y.W. Kim and W.M. Griffith (editors), 1988, pp. 323-336.
- [10] ASTM, *Annual Book of ASTM Standards*, Vol. 3.01, E647, "Standard Test Method for Measurement of Fatigue Crack Growth Rates," American Society for Testing and Materials, West Conshohocken, PA, 2001.
- [11] R. S. Piascik, J. C. Newman, Jr., and J. H. Underwood, "The Extended Compact Tension Specimen," *Fatigue and Fracture of Engineering Materials and Structures*, Vol. 20, 1997, pp. 559-563.
- [12] J. K. Donald, G. Bray, and R. Bush, "Introducing the K_{\max} Sensitivity Concept for Correlating Fatigue Crack Growth Data," *High Cycle Fatigue of Structural Materials*, W.O. Soboyejo and T.S. Srivatsan (editors), 1997, The Minerals, Metals, and Materials Society, pp. 123-141.

REPORT DOCUMENTATION PAGE			Form Approved OMB No. 0704-0188	
Public reporting burden for this collection of information is estimated to average 1 hour per response, including the time for reviewing instructions, searching existing data sources, gathering and maintaining the data needed, and completing and reviewing the collection of information. Send comments regarding this burden estimate or any other aspect of this collection of information, including suggestions for reducing this burden, to Washington Headquarters Services, Directorate for Information Operations and Reports, 1215 Jefferson Davis Highway, Suite 1204, Arlington, VA 22202-4302, and to the Office of Management and Budget, Paperwork Reduction Project (0704-0188), Washington, DC 20503.				
1. AGENCY USE ONLY (Leave blank)		2. REPORT DATE May 2002		3. REPORT TYPE AND DATES COVERED Technical Memorandum
4. TITLE AND SUBTITLE Accelerated Near-Threshold Fatigue Crack Growth Behavior of an Aluminum Powder Metallurgy Alloy			5. FUNDING NUMBERS WU 706-62-31-01	
6. AUTHOR(S) Robert S. Piascik and John A. Newman				
7. PERFORMING ORGANIZATION NAME(S) AND ADDRESS(ES) NASA Langley Research Center Hampton, VA 23681-2199 U.S. Army Research Laboratory Vehicle Technology Directorate NASA Langley Research Center Hampton, VA 23681-2199			8. PERFORMING ORGANIZATION REPORT NUMBER L-18180	
9. SPONSORING/MONITORING AGENCY NAME(S) AND ADDRESS(ES) National Aeronautics and Space Administration Washington, DC 20546-0001 and U.S. Army Research Laboratory Adelphi, MD 20783-1145			10. SPONSORING/MONITORING AGENCY REPORT NUMBER NASA/TM-2002-211676 ARL-TR-2728	
11. SUPPLEMENTARY NOTES				
12a. DISTRIBUTION/AVAILABILITY STATEMENT Unclassified-Unlimited Subject Category 26 Availability: NASA CASI (301) 621-0390 Distribution: Nonstandard			12b. DISTRIBUTION CODE	
13. ABSTRACT (Maximum 200 words) Fatigue crack growth (FCG) research conducted in the near threshold regime has identified a room temperature creep crack growth damage mechanism for a fine grain powder metallurgy (PM) aluminum alloy (8009). At very low DK, an abrupt acceleration in room temperature FCG rate occurs at high stress ratio ($R = K_{min}/K_{max}$). The near threshold accelerated FCG rates are exacerbated by increased levels of K_{max} ($K_{max} < 0.4 KIC$). Detailed fractographic analysis correlates accelerated FCG with the formation of crack-tip process zone microvoid damage. Experimental results show that the near threshold and K_{max} influenced accelerated crack growth is time and temperature dependent.				
14. SUBJECT TERMS Aluminum alloy 8009, Powder metallurgy, Fatigue crack growth, K_{max} , Room-temperature creep			15. NUMBER OF PAGES 11	
			16. PRICE CODE	
17. SECURITY CLASSIFICATION OF REPORT Unclassified	18. SECURITY CLASSIFICATION OF THIS PAGE Unclassified	19. SECURITY CLASSIFICATION OF ABSTRACT Unclassified	20. LIMITATION OF ABSTRACT UL	